



## RESEARCH ARTICLE

# Novel 5-(1-aryl-1*H*-pyrazol-3-yl)-1*H*-tetrazoles as glycogen phosphorylase inhibitors: An in vivo antihyperglycemic activity study

Pramod P. Kattimani<sup>1</sup> | Shilpa M. Somagond<sup>1</sup> | Praveen K. Bayannavar<sup>1</sup> |  
Ravindra R. Kamble<sup>1</sup> | Subhas C. Bijjaragi<sup>2</sup> | Raveendra K. Hunnur<sup>3</sup> |  
Shrinivas D. Joshi<sup>4</sup>

<sup>1</sup>Department of Studies in Chemistry, Karnatak University, Dharwad, Karnataka, India

<sup>2</sup>Department of Studies in Zoology, Karnatak University, Dharwad, Karnataka, India

<sup>3</sup>APL Research Ltd., Batchupally, Telangana, India

<sup>4</sup>Novel Drug Design and Discovery Laboratory, Department of Pharmaceutical Chemistry, S.E.T.'s College of Pharmacy, Dharwad, Karnataka, India

**Correspondence**

Ravindra R. Kamble, Department of Studies in Chemistry, Karnatak University, Dharwad 580003, Karnataka, India.  
Email: kamchem9@gmail.com

**Funding information**

University Grants Commission

**Abstract**

In this study, we report the ring transformation of 3-arylsydnone into 1-aryl-1*H*-pyrazole-3-carbonitriles via [3 + 2] cycloaddition with acrylonitrile. 1-Aryl-1*H*-pyrazole-3-carbonitrile underwent [2 + 3] cycloaddition with sodium azide to afford 5-(1-aryl-1*H*-pyrazol-3-yl)-1*H*-tetrazoles which were further subjected to *N*-alkylation with aryl/heteroaryl alkyl halides to afford 1,5- and 2,5-disubstituted tetrazoles. Furthermore, the title compounds were screened for in vivo antihyperglycemic activity using albino Wistar rats of either sex. Compounds **4a**, **6b**, **7a**, **7b**, **8b**, and **9b** showed maximum fall in the blood glucose levels in streptozotocin-induced diabetic rats after 5–7 days of administration. In support of antidiabetic activity, we also performed the experimental in vivo studies, namely, effect of compounds on enzymes (serum glutamic oxaloacetic transaminase, serum glutamic-pyruvic transaminase, creatinine, urea, and total protein), antihyperlipidemic, and histopathology. Moreover, the molecular docking study has been performed for potent molecules among the series with glycogen phosphorylase as target enzyme, and this study corroborated the experimental in vivo results.

**KEYWORDS**

3-arylsydnone, glycogen phosphorylase, in vivo antihyperglycemic activity

## 1 | INTRODUCTION

Diabetes is one of the foremost serious life style disorder and metabolic chronic disease that has attacked the world at an alarming wide spread rate. It is characterized by high blood glucose level due to the defects in insulin secretion or insulin action or both (Matschinsky, 1996). A survey from the International Diabetes Federation (IDF) reveals that diabetes has affected approximately 425 million individuals in 2017, and this range is anticipated to rise to 629 million by 2045 (IDF Diabetes Atlas, 2018). It is grouped as Type 1 and Type 2 that happened due to insulin resistance in body tissues, and its

prevalence is driven by several factors such as diet, obesity, stress, urbanization, and lack of physical activity (World Health Organization, 2016). Type 2 diabetes mellitus (T2DM) is a severe sickness with giant economic consequences, which is considerably underdiagnosed and incompletely treated within the general population (Zimmet, Alberti, & Shaw, 2001; Diamond (2003). In the treatment of diabetic patients, control of blood sugar levels is a key factor and these patients are most frequently prescribed with modification of diet and exercise, one or more oral hypoglycemic agents, as well as insulin. In spite of the provision of various categories of hypoglycemic medicine, present treatments are often unable to attain an intensive degree of blood

sugar management to cut back effectively the occurrence and brutality of diabetic complications (Wagman & Nuss, 2001).

In Type 2 diabetic patients, the hepatic glucose output is increased and the current evidence indicates that abnormal high production of glucose by liver is due to the glycogenolysis (release of monomeric glucose from the glycogen polymer storage form). One of the pharmacological approaches to reduce this elevated hepatic glucose in Type 2 diabetes is to inhibit glycogen phosphorylase (GP) enzyme (Baker, Greenhaff, & Timmons, 2006; Henke & Sparks, 2006; Loughlin, 2010; Oikonomakos, 2002; Oikonomakos & Somsák, 2008; Somsak et al., 2008). GP is primarily expressed in the liver and is responsible for glycogen breakdown to release glucose and connected metabolites for energy supply (glycogenolysis), thus inhibiting GP will limit glycogenolysis and subordinate hepatic glucose production (Kurukulasuriya et al., 2003). Hence, GP is a molecular therapeutic target for treating hyperglycemia associated with T2DM (Henke & Sparks, 2006; Hoover et al., 1998; Oikonomakos, 2002; Somsak et al., 2008; Treadway, Mendys, & Hoover, 2001).

The occurrence of a heterocycle functioning as central part of drug molecules is an incident that takes place commonly in many natural and synthetic drug molecules. Particularly, five- and six-membered heterocyclic systems are motifs of many efficacious drugs (Figure 1). Pyrazoles are well-known examples of aromatic five-membered heterocyclic organic compounds containing two adjacent nitrogen atoms endowed with diverse biological activity on humans such as antimicrobial (Sridhar et al., 2004), antidiabetic, anticancer (Altintop, Ozdemir, Ilgin, & Atli, 2014), anti-inflammatory (Raffa et al., 2010; Ren et al., 2018), antiviral (El-Sabbagh et al., 2009), anticonvulsant, and antidepressant (Abdel-Aziz, El-Din, Abu-Rahma, & Hassan, 2009). Furthermore, the pyrazole derivatives are used as synthon for the development of condensed heterocyclic scaffolds and thus signify as interesting template for combinational chemistry (Singh, Paul, & Holzer, 2006; Tiwari, Ameta, Ranwal, Ameta, & Punjabi, 2013). Pyrazole-containing remogliflozin etabonate is found to lower the blood glycemic levels and is now under clinical trials (Fujimori et al., 2008).

5-Substituted-1H-tetrazoles serve as nonclassical isostere for the carboxylic acid moiety (RCO<sub>2</sub>H) in biologically active molecules (Butler, 1996; Le Bourdonnec et al., 2000; Lipinski, 1986; Nisa et al., 2015; Sharon et al., 2005a, 2005b; Subramanian et al., 2015;

Wittenberger, 1994). However, 1,5-disubstituted tetrazoles can be used as isosteres of *cis*-amide bond of peptides (May & Abell, 2001; May & Abell, 2002). Substances containing 1,5-disubstituted tetrazole fragment are being well studied as they exhibit anti-inflammatory (Rajasekaran & Thampi, 2004), antiviral, (Muraglia et al., 2006), antitubercular (Karabanovich et al., 2015), anticonvulsant, antimicrobial (Rostom, Ashour, Abd El Razik, Abd El Fattah, & El-Din, 2009), antiparasitic (Pedro et al., 2014), antiulcer (Uchida et al., 1989), antihypertensive (Ashton et al., 1992), antimalarial (Pandey et al., 2013), anticancer (Arshad et al., 2014), and COX-2 inhibitory (Al-Hourani et al., 2011) properties. 2,5-Disubstituted tetrazoles have been proved to exhibit antiviral (Chang et al., 2005), antimicrobial (Rostom, Ashour, Abd El Razik, Abd El Fattah, & El-Din, 2009), and glutamate receptor modulating (Vieira et al., 2005) properties. Synthesized tetrazole having *N*-glycosides as SGLT2 inhibitors and evaluated for their hypoglycemic effects in vivo by mice oral glucose tolerance test (Gao et al., 2010). 1-[5-[(4-Ethoxyphenyl)methyl]-2H-tetrazol-2-yl]-1-deoxy-β-D-glycopyranose **4** was found to be most active against standard drug Dapagliflozin **6** (Gao et al., 2010). Vieira et al. (2005) reported a new series of 5-[(5-aryl-1H-pyrazol-3-yl) methyl]-1H-tetrazoles **5** and evaluated for their in vivo antihyperglycemic activity by sucrose loaded model. These compounds showed significant antihyperglycemic activity (Sharon et al., 2005a, 2005b) (Figure 2).

3-Arylsydnone undergo ring transformation reactions yielding pharmaceutically important heterocycles (Angadiyavar & George, 1971; Browne & Harrity, 2010; Mallur & Badami, 2000; Wu, Fang, Larock, & Shi, 2010). This fact has triggered sydnone as the prominent synthon among all the mesoionic compounds. In view of this, we have attempted [3 + 2] cycloaddition reaction of 3-arylsydnone with acrylonitrile to afford 1-aryl-1H-pyrazole-3-carbonitrile (**2a-c**) which served as dipolarophile for subsequent [3 + 2] cycloaddition with sodium azide to get 5-(1-aryl-1H-pyrazol-3-yl)-1H-tetrazoles (**3a-c**). Tetrazole derivative **3a-c** was then subjected to *N*-alkylation with aryl/heteroaryl alkyl halides (**i-iv**) in the presence of anhydrous potassium carbonate to get the title Compounds **4-9 (a-d)** (Scheme 1). The title Compounds **4-9 (a-d)** were further evaluated for in vivo antihyperglycemic activity using Wistar albino rats of either sex and carried out the histopathological, biochemical parameters, and lipid profile studies.

## 2 | METHODS

### 2.1 | X-ray diffraction studies

Single-crystal X-ray diffraction (XRD) study was carried out for Compound **4b**. Data collection: SMART (Bruker, 2001); cell refinement: SAINT (Bruker, 2001); data reduction: SAINT; program(s) used to solve structure: SHELXS97 (Sheldrick, 1997); molecular graphics: ORTEP-3 (Farrugia, 2012); software used to prepare material for publication: SHELXL97 (Sheldrick, 1997). The ORTEP, unit cell, hydrogen bonding, dihedral angles, and packing diagrams were obtained by MERCURY software.

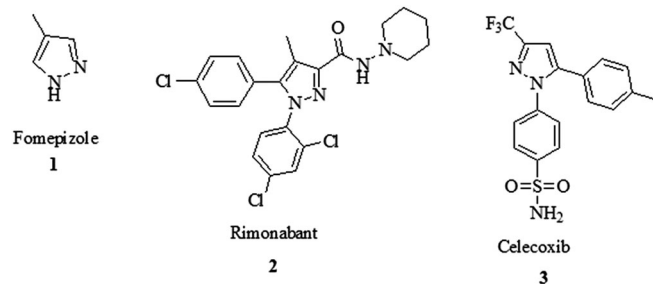
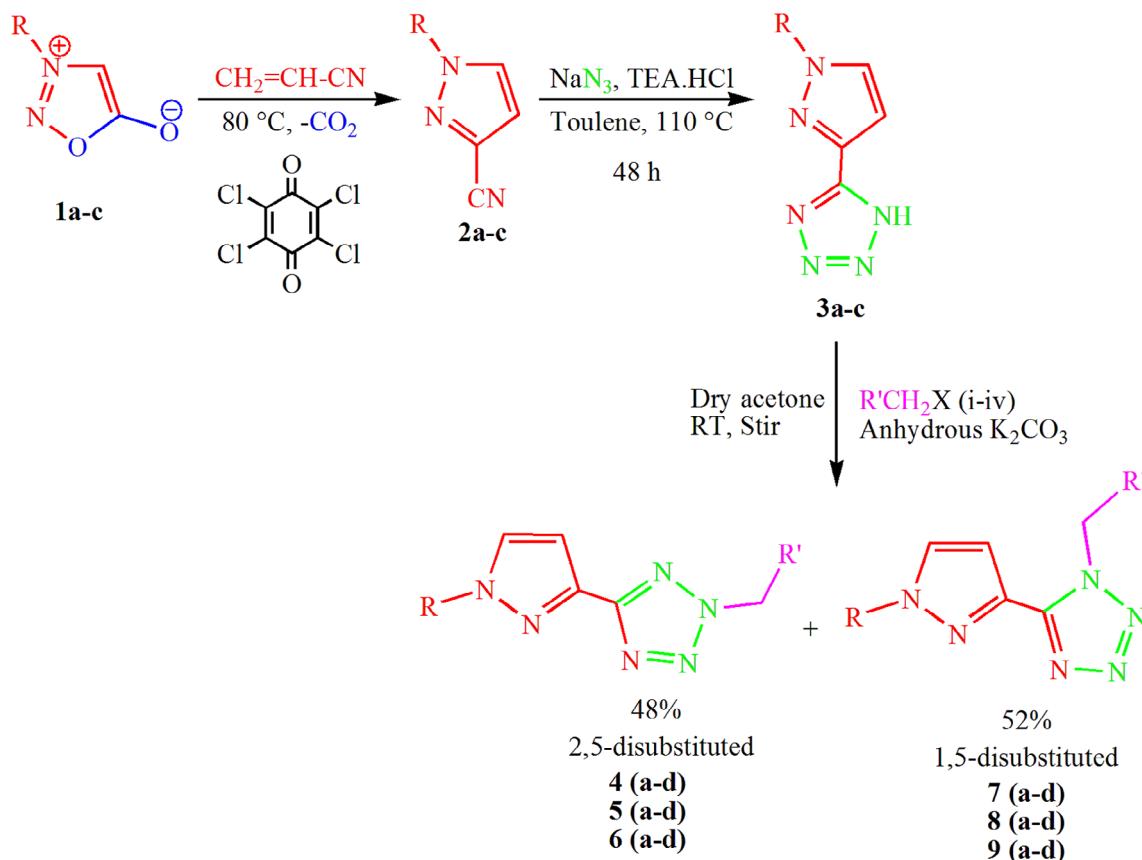
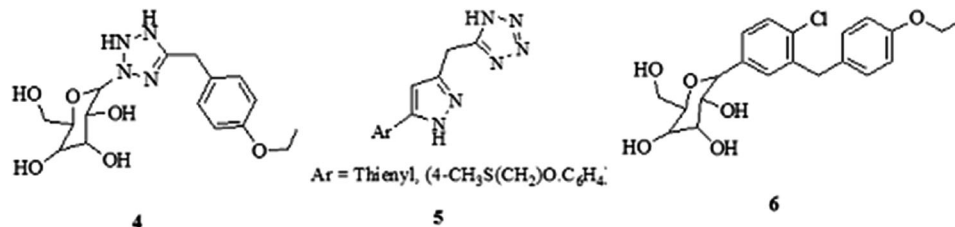


**FIGURE 1** Several drug molecules that include pyrazole as a core moiety

**FIGURE 2** Some examples of tetrazole-bearing potent antihyperglycemic-reported molecules



**SCHEME 1** Synthetic route for the title Compounds 4–7 (a–d)

## 2.2 | In vivo antihyperglycemic assay

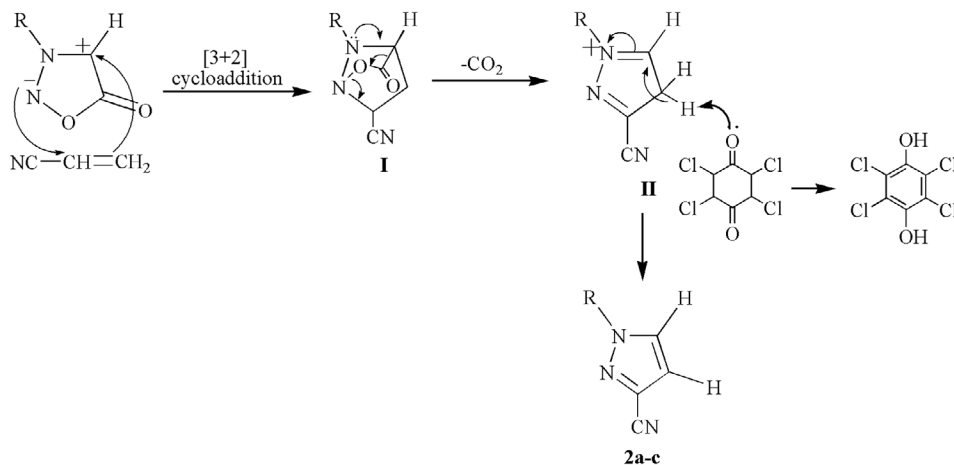
### 2.2.1 | Streptozotocin-induced diabetic rat model

Animals were supplied by the Department of Zoology, Karnatak University, Dharwad, Karnataka, India, and the animal house registration number is 639/02/A/CPCSEA, dated: July 19, 2002. Diabetes was induced in fasted rats (12 hr) by intraperitoneal injection of streptozotocin monohydrate at 120 mg/kg body weight (b.w.) dissolved in 0.90 M saline. Food was provided 30 mins after the administration of streptozotocin. Diabetes was confirmed 48 hr later by glucometer (One Touch Ultra, Johnson & Johnson Co. LifeScan Scotland Ltd., Beechwood Park North, Inverness IV2 3ED, UK) using tail vein blood sample. Animals with a blood glucose level above 200 mg/dL were considered diabetic and were included in the experiment.

### 2.2.2 | Experimental protocols

The animals were further divided into 10 groups of 6 animals each as follows:

- Group I:** Normal (vehicle).
- Group II:** Dimethylsulphoxide (DMSO) control (0.2 ml).
- Group III:** Diabetic control.
- Group IV:** Diabetic animals treated with glibenclamide (0.25 mg/kg b.w.).
- Group V:** Diabetic animals treated with 4a (100 mg/kg b.w. in 0.2 ml DMSO).
- Group VI:** Diabetic animals treated with 6b (100 mg/kg b.w. in 0.2 ml DMSO).
- Group VII:** Diabetic animals treated with 7a (100 mg/kg b.w. in 0.2 ml DMSO).



**Group VIII:** Diabetic animals treated with **7b** (100 mg/kg b.w. in 0.2 ml DMSO).

**Group IX:** Diabetic animals treated with **8b** (100 mg/kg b.w. in 0.2 ml DMSO).

**Group X:** Diabetic animals treated with **9b** (100 mg/kg b.w. in 0.2 ml DMSO).

Animals of **Group I** were untreated and considered as normal control. Animals of **Group II** were given an equal amount of DMSO. Compounds **4**, **5**, **6**, **7**, **8**, and **9** (a-d) and glibenclamide were orally administered through gavage daily for 28 days. The blood glucose level of treated **Groups IV-X** was determined at 30, 60, 90, 120, 180, and 240 min and 12 hr using glucometer on the first day of administration of synthesized compounds. From second day onwards, the blood glucose level was determined at every 6-hr time interval for 28 days. Animals not found diabetic after 24-h posttreatment with streptozotocin were not considered and omitted from the calculations. The treated compounds that did not show any fall in the blood glucose level of animals were also omitted from the calculations and considered as inactive. Food but not water was withheld from the cages at the time of experiment.

At the end of experimental period (28 days), the animals were fasted overnight and the blood sample of experimental animals was withdrawn through retro-orbital plexus puncture. The serum was separated by centrifuging at 3000 rpm for 20 min and used for various biochemical estimations.

### 2.2.3 | Biochemical parameters

The blood serum creatinine, urea, and total protein were estimated according to the standardized procedures. The serum lipid profiles such as total cholesterol (TC), triglyceride (TG), and high-density lipoprotein (HDL) were estimated using commercially available kits (Accurex Biomedicals, Pvt. Ltd., Mumbai, India). The serum low-density lipoprotein (LDL) and very low-density lipoprotein (VLDL) were calculated using Friedewald formula (Friedewald, Levy, & Fredrickson, 1972). Serum glutamic oxaloacetic transaminase (SGOT) and serum glutamic-pyruvic transaminase (SGPT) activities were determined by the method developed by Reitman and Frankel (1957).

### 2.2.4 | Tissue preparation

Animals of all the groups were sacrificed by the administration of 40 mg/kg b.w. pentobarbital and dissected to get pancreas tissue for histopathological studies. The collected tissues were preserved in 4% paraformaldehyde for 48 hr and then dehydrated sequentially in gradient ethanol-water (50, 70, 80, 90, and 95%, and finally in 100% alcohol). Samples were immersed in xylene for 30 min and incubated with paraffin at 65 °C overnight. After embedding in wax, tissues were cut into ultrathin sections of 5 μm thickness by Leica RM 2255 microtome (Leica, Nussloch, Germany) and spread on the glass slides. Sections were deparaffinated with fresh xylene for 30 min, hydrated with gradient ethanol (100, 90, 80, and 70%), and then washed with double distilled water for three times. The sections were stained with hematoxylin and eosin and mounted in deparaffinated xylene for the observation of microscopic cells for necrosis, fat degradation, and pancreatic degeneration. The sections were examined and micrographs were captured using Axio Imager M.2 microscope for histological evaluation.

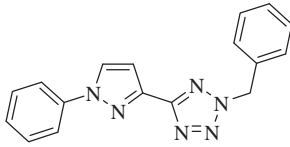
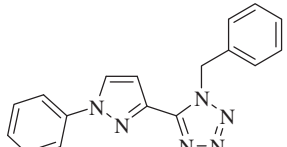
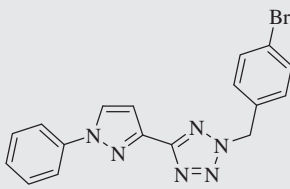
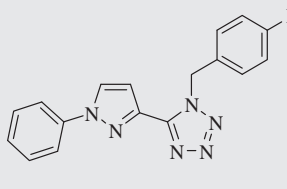
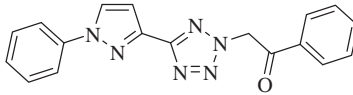
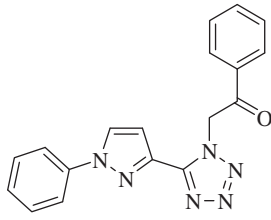
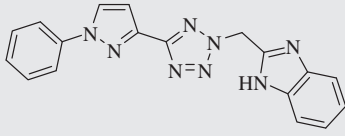
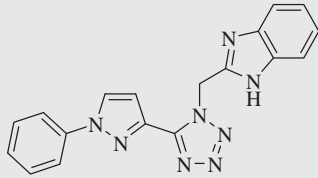
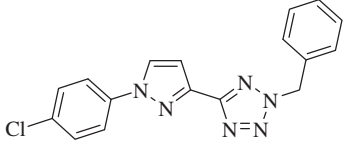
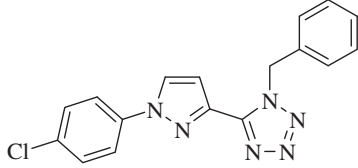
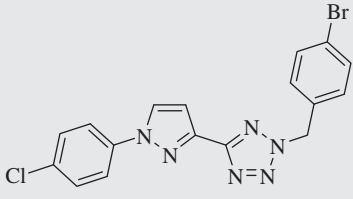
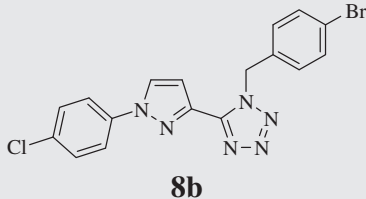
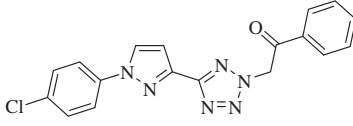
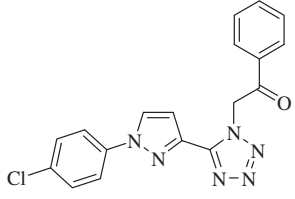
### 2.2.5 | Statistical analysis

All the values were expressed as mean ± SE. One-way analysis of variance was used to detect statistical significance followed by post hoc multiple comparisons (Tukey's test). A value of  $p < .05$  was considered to be significant.

## 2.3 | Docking simulation

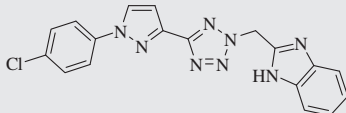
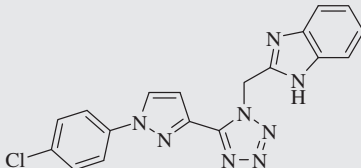
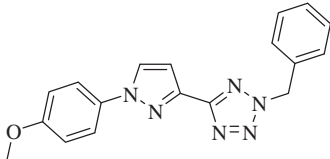
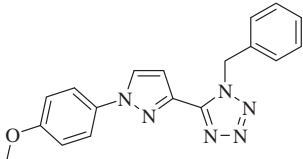
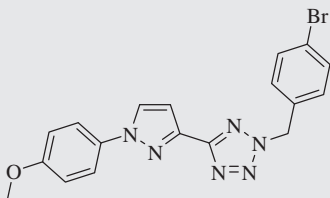
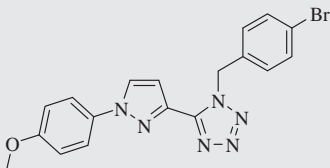
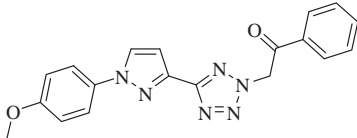
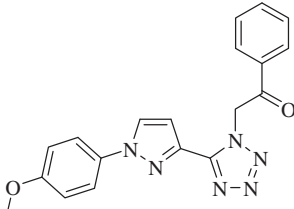
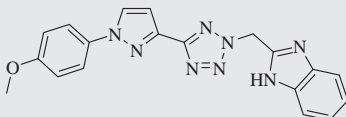
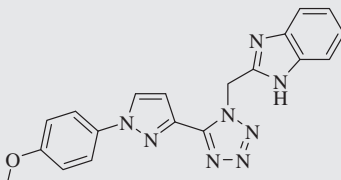
The crystal structure used was that of human liver GP, complexed with caffeine, *N*-acetyl-beta-D-glucopyranosylamine, and CP-403700 (Protein Data Bank [PDB] ID: 1L5Q; B chain) for docking studies, obtained from the PDB. The protein was designed for docking by adding polar hydrogen atom with the Gasteiger-Huckel charges (Gasteiger and Marsili, 1980) and water molecules were removed. The three-dimensional structure of the ligands was generated by the SKETCH module implemented in the SYBYL program (Tripos Inc., St. Louis, MO) and its energy-minimized conformation was obtained with the help of the Tripos force field using the

**TABLE 1** Structures of the synthesized compounds

Sl. no.	R	R'	2,5-Disubstituted compound	1,5-Disubstituted compound
1	C <sub>6</sub> H <sub>5</sub>	C <sub>6</sub> H <sub>5</sub>		
2	C <sub>6</sub> H <sub>5</sub>	<i>p</i> -BrC <sub>6</sub> H <sub>4</sub>		
3	C <sub>6</sub> H <sub>5</sub>	C <sub>6</sub> H <sub>4</sub> CO		
4	C <sub>6</sub> H <sub>5</sub>	benzimidazol-2-yl		
5	<i>p</i> -ClC <sub>6</sub> H <sub>4</sub>	C <sub>6</sub> H <sub>5</sub>		
6	<i>p</i> -ClC <sub>6</sub> H <sub>4</sub>	<i>p</i> -BrC <sub>6</sub> H <sub>4</sub>		
7	<i>p</i> -ClC <sub>6</sub> H <sub>4</sub>	C <sub>6</sub> H <sub>4</sub> CO		

(Continues)

**TABLE 1** (Continued)

Sl. no.	R	R'	2,5-Disubstituted compound	1,5-Disubstituted compound
8	<i>p</i> -ClC <sub>6</sub> H <sub>4</sub>	Benzimidazol-2-yl		
9	<i>p</i> -CH <sub>3</sub> O-C <sub>6</sub> H <sub>4</sub>	C <sub>6</sub> H <sub>5</sub>		
10	<i>p</i> -CH <sub>3</sub> O-C <sub>6</sub> H <sub>4</sub>	<i>p</i> -BrC <sub>6</sub> H <sub>4</sub>		
11	<i>p</i> -CH <sub>3</sub> O-C <sub>6</sub> H <sub>4</sub>	C <sub>6</sub> H <sub>4</sub> CO		
12	<i>p</i> -CH <sub>3</sub> O-C <sub>6</sub> H <sub>4</sub>	Benzimidazol-2-yl		

Gasteiger-Huckel charges, and molecular docking was performed with Surflex-Dock program that is interfaced with Sybyl-X 2.0 (Tripos International, 2012), and other miscellaneous parameters were assigned with the default values given by the software.

### 3 | RESULTS AND DISCUSSION

#### 3.1 | Chemistry

To start with, 3-arylsydnone (**1a–c**) was ring transformed into 1-aryl-1*H*-pyrazole-3-carbonitrile (**2a–c**) via [3 + 2] dipolar cycloaddition with acrylonitrile in the presence of chloranil. The reaction was initiated with the loss of carbon dioxide (**I**) followed by rearomatization of intermediate by

chloranil (**II**) resulting in the formation of **2a–c** (Scheme 2). The obtained 1-aryl-1*H*-pyrazole-3-carbonitrile (**2a–c**) was subjected to [3 + 2] cycloaddition with sodium azide in the presence of triethylamine hydrochloride to afford corresponding 5-(1-aryl-1*H*-pyrazol-3-yl)-1*H*-tetrazole (**3a–c**).

It is well known that 5-substituted-1*H*-tetrazole (RCHN<sub>4</sub>) containing a free N–H bond exists mainly in 1*H*– and 2*H*– tautomeric forms. Consequently, *N*-alkylation of 5-(1-aryl-1*H*-pyrazol-3-yl)-1*H*-tetrazole (**3a–c**) with aryl/heteroaryl alkyl halides (i–iv) in the presence of anhydrous potassium carbonate afforded two regioisomers, namely, 2,5-disubstituted (**4–6** [a–d]) and 1,5-disubstituted (**7–9** [a–d]) tetrazoles nearly in 1:1 ratio. These regioisomers were successfully separated by column chromatographic technique using hexane:ethylacetate (9:1) solvent mixture as an eluent. All the synthesized

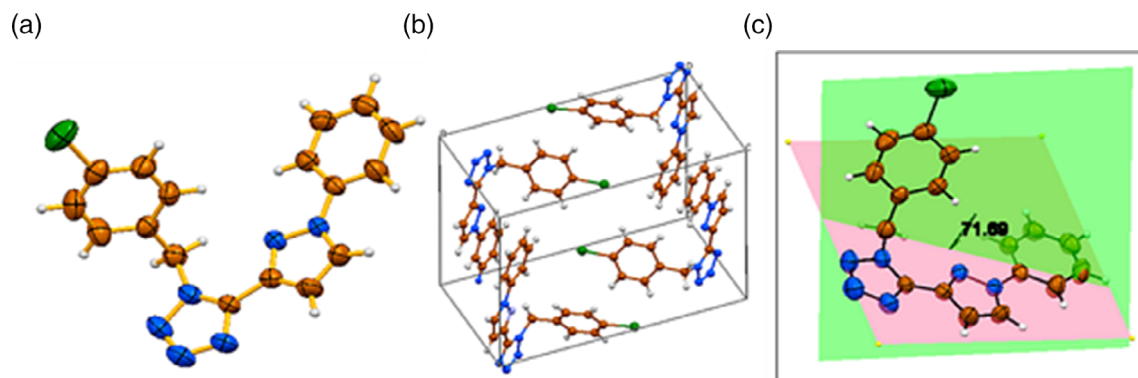


**FIGURE 3** (a) Molecular structure of Compound **4b**; displacement ellipsoids are drawn at the 50% probability. (b) Unit cell packing diagram of the molecules of **4b**; hydrogen atoms are shown as sphere of arbitrary radius. (c) Planes of the molecule **4b**

**TABLE 2** In silico pharmacokinetics data of the title Compounds **4a–d**, **5a–d**, **6a–d**, and **7a–d** as predicted by Molsoft and admet SAR online servers

Entry no.	Log <i>P</i> < 5 <sup>a</sup>	Molecular weight < 500 amu <sup>b</sup>	Hydrogen Bond Acceptor (accptHB) < 10 <sup>c</sup>	Hydrogen Bond Donor (donorHB) < 5 <sup>d</sup>	Lipinsk's violation	Topological polar surface area (TPSA) < 140 Å <sup>e</sup>	Drug likeliness score	Blood Brain Barrier permeability	Probability
<b>4a</b>	3.26	302.13	4	0	0	52.58	-0.69	+	.98
<b>4b</b>	4.11	380.04	4	0	0	52.58	-0.58	+	.98
<b>4c</b>	2.61	330.12	5	0	0	65.83	-0.77	+	.99
<b>4d</b>	2.67	342.13	5	1	0	72.86	-0.54	+	.98
<b>5a</b>	3.97	336.09	4	0	0	52.58	-0.44	+	.98
<b>5b</b>	4.83	414.00	4	0	0	52.58	-0.92	+	.98
<b>5c</b>	3.32	364.08	5	0	0	65.83	-0.51	+	.98
<b>5d</b>	3.38	376.10	5	1	0	72.86	-0.16	+	.97
<b>6a</b>	3.35	332.14	5	0	0	60.13	-0.70	+	.99
<b>6b</b>	4.20	410.05	5	0	0	60.13	-0.64	+	.98
<b>6c</b>	2.70	360.13	6	0	0	73.37	-0.69	+	.98
<b>6d</b>	2.76	372.14	6	1	0	80.41	-0.43	+	.98
<b>7a</b>	2.86	302.13	4	0	0	53.41	-0.69	+	.98
<b>7b</b>	3.71	380.04	4	0	0	53.41	-0.58	+	.98
<b>7c</b>	2.21	330.12	5	0	0	66.66	-0.77	+	.98
<b>7d</b>	2.27	342.13	5	1	0	73.69	-0.54	+	.98

<sup>a</sup>Logarithm of partition coefficient.

<sup>b</sup>Atomic Mass Unit.

<sup>c</sup>Hydrogen Bond Acceptor.

<sup>d</sup>Hydrogen Bond Donor.

<sup>e</sup>Topological Polar Surface Area.

compounds (Table 1) were characterized by <sup>1</sup>H NMR, <sup>13</sup>C NMR, mass spectral, and elemental analyses. And also we have carried out the single-crystal XRD studies for Compound **4b**.

In case of <sup>1</sup>H NMR analysis, the C5 proton of pyrazole ring has resonated as doublet in the range  $\delta$  7.82–8.74 ppm, whereas the C4 proton of pyrazole ring has resonated as doublet at  $\delta$  6.98–7.25 ppm. The C5 carbon of tetrazole ring showed signals between  $\delta$  159 and  $\delta$  161 ppm. The signal in the range  $\delta$  141–142 ppm was attributed to C3 carbon of pyrazole ring of 2,5-disubstituted tetrazoles and  $\delta$

148–149 ppm for 1,5-disubstituted tetrazoles. The C5 and C4 carbons of pyrazole ring gave signals around  $\delta$  126–128 and  $\delta$  107–109 ppm, respectively. It was interesting to know that both 2,5- and 1,5-disubstituted tetrazole derivatives showed slightly different chemical shift values particularly for the methylene group. Methylene protons in the case of 2,5-disubstituted tetrazoles were resonated at slightly upfield values in the range  $\delta$  5.77–6.22 ppm when compared to 1,5-disubstituted tetrazole derivatives which have shown signals at  $\delta$  6.05–6.28 ppm. In case of <sup>13</sup>C NMR, the methylene carbon of

Entry	0 hr	Day 1	Day 2	Day 3	Day 4	Day 5	Day 6	Day 7
Control	95	107	123	101	97	114	102	117
Diabetic	440	434	430	455	457	441	446	447
4a	425	397	382	327	255	181	154	126
4b	444	434	418	426	431	411	427	416
4c	390	405	402	397	415	407	408	401
4d	393	397	386	400	404	397	398	402
5a	417	423	417	419	421	422	425	428
5b	419	421	429	418	420	418	417	419
5c	399	409	415	401	399	412	411	406
5d	454	461	458	460	456	452	457	455
6a	400	397	389	404	406	404	401	402
6b	387	360	348	311	273	178	144	113
6c	398	392	396	399	405	410	406	401
6d	378	387	390	394	389	386	390	392
7a	460	434	412	367	359	311	230	144
7b	396	384	376	342	327	272	220	137
7c	472	477	475	466	469	471	472	475
7d	450	448	449	451	457	463	458	460
8a	382	386	389	384	386	382	389	386
8b	425	402	390	365	337	315	245	151
8c	367	378	395	409	411	415	410	406
8d	411	407	400	398	412	417	410	416
9a	409	415	414	409	417	420	423	425
9b	444	418	390	363	334	300	221	138
9c	395	397	388	392	391	390	395	392
9d	393	399	404	395	383	393	399	395
G	400	380	320	210	171	155	142	131

**TABLE 3** Blood glucose level (mg/dl) of each group

Note: G represents glibenclamide.

**TABLE 4** Effect of compounds on biochemical parameters

Groups/parameter	SGOT	SGPT	Creatinine	Urea	Total protein
Control	130.33 ± 1.05	82.50 ± 0.98	0.73 ± 0.35	36.23 ± 0.59	7.99 ± 0.27
Diabetic	214.33 ± 1.81	161.50 ± 2.18	2.41 ± 0.170	86.48 ± 1.21	4.75 ± 0.17
4a	165.00 ± 3.72	117.51 ± 1.43	1.41 ± 0.598	65.10 ± 1.25	5.57 ± 0.13
6b	152.33 ± 1.99	106.34 ± 1.47	1.00 ± 0.027	61.33 ± 0.63	5.40 ± 0.20
7a	138.34 ± 1.45	105.52 ± 1.61	0.98 ± 0.028	55.75 ± 0.94	6.24 ± 0.65
7b	145.02 ± 1.91	94.33 ± 1.12	1.16 ± 0.148	63.16 ± 0.92	6.15 ± 0.07
8b	149.17 ± 1.78	105.02 ± 1.06	1.15 ± 0.155	65.83 ± 0.62	6.32 ± 0.11
9b	155.82 ± 2.41	108.01 ± 2.04	0.90 ± 0.030	65.32 ± 0.61	6.72 ± 0.21

Note: The data represent the mean ± SE (n = 6).

Abbreviations: SGOT, serum glutamic oxaloacetic transaminase; SGPT, serum glutamic-pyruvic transaminase.

2,5-disubstituted tetrazoles gave signals at  $\delta$  46–57 ppm, while 1,5-disubstituted tetrazoles gave signals at  $\delta$  49–56 ppm. All other signals were in accordance with the proposed structures. The mass spectral analysis of all the title compounds has shown the  $m/z$  values which correspond to their molecular mass.

### 3.2 | X-ray crystallographic structure analysis of 4b

Crystals of Compound **4b** were developed by slow evaporation of dry acetone at room temperature. The asymmetric unit of Compound **4b** is shown in Figure 3b. The dihedral angle (Figure 3c) between

tetrazole ring and pyrazole and two terminal benzene rings of molecules are  $4.21^\circ$ ,  $71.69^\circ$ ,  $4.76^\circ$ , respectively. In the structure, all bond lengths and angles are within normal the range (Zhang, 2009). The crystal structure is further stabilized by intermolecular C—H...N and intramolecular C—H...N hydrogen bonds (Figure 3).

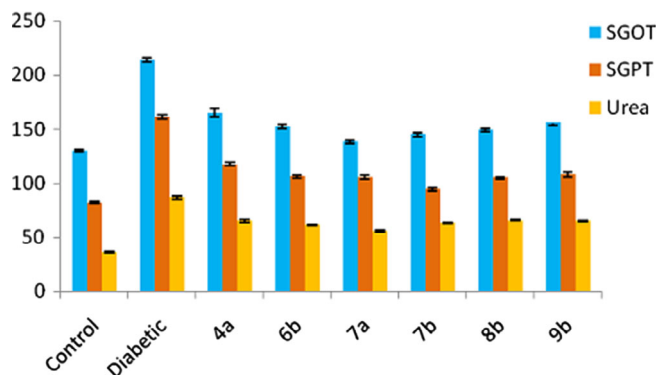


**FIGURE 4** Effect of compounds on SGOT, SGPT, and urea. Values are given as mean  $\pm$  SE. SGOT, serum glutamic oxaloacetic transaminase; SGPT, serum glutamic-pyruvic transaminase

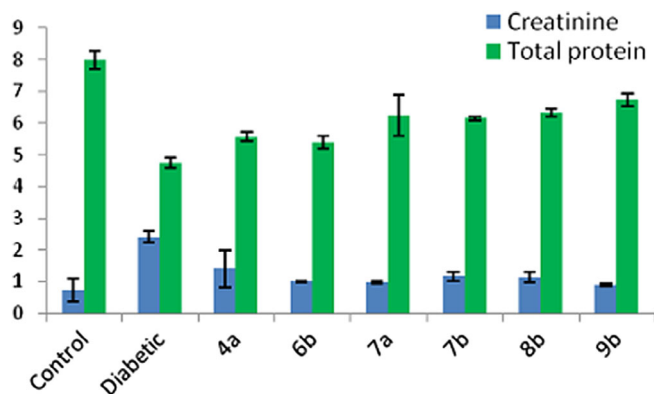


**FIGURE 5** Effect of compounds on creatinine and total protein parameters. Values are given as mean  $\pm$  SE

**TABLE 5** Effect of compounds on lipid profile

Groups/parameters	TC	TG	HDL	LDL	VLDL
Control	133.50 $\pm$ 1.11	114.17 $\pm$ 1.40	58.10 $\pm$ 0.55	76.33 $\pm$ 0.96	45.19 $\pm$ 0.82
Diabetic	259.83 $\pm$ 5.44	184.83 $\pm$ 2.93	29.58 $\pm$ 1.56	259.33 $\pm$ 3.97	86.16 $\pm$ 1.04
4a	185.11 $\pm$ 4.17	155.33 $\pm$ 2.83	34.50 $\pm$ 1.47	158.67 $\pm$ 5.70	58.00 $\pm$ 1.54
6b	164.33 $\pm$ 2.61	144.50 $\pm$ 2.45	45.16 $\pm$ 1.35	143.50 $\pm$ 1.36	63.50 $\pm$ 2.55
7a	146.17 $\pm$ 3.02	139.40 $\pm$ 4.37	45.83 $\pm$ 2.08	106.17 $\pm$ 1.19	64.66 $\pm$ 0.88
7b	152.67 $\pm$ 1.49	136.67 $\pm$ 2.10	52.50 $\pm$ 1.23	106.17 $\pm$ 1.66	72.50 $\pm$ 1.23
8b	148.50 $\pm$ 1.91	132.83 $\pm$ 1.77	45.33 $\pm$ 1.60	113.33 $\pm$ 0.88	62.50 $\pm$ 1.87
9b	146.17 $\pm$ 2.13	144.17 $\pm$ 2.65	46.83 $\pm$ 1.16	114.83 $\pm$ 1.88	62.00 $\pm$ 1.36

Note: The data represent the mean  $\pm$  SE ( $n = 6$ ).

Abbreviations: HDL, high-density lipoprotein; LDL, low-density lipoprotein; TC, total cholesterol; TG, triglyceride; VLDL, very low-density lipoprotein.

### 3.3 | Pharmacology

#### 3.3.1 | Drug likeliness parameters

To be an effective antidiabetic drug, the candidate compounds must be able to cross the Blood Brain Barrier (BBB) to exert their action. They should also possess good pharmacokinetic and oral bioavailability properties (Kothayer, Ibrahim, Soltan, Rezq, & Mahmoud, 2018). The drug-like properties of the designed compounds were predicted using the web tool Molinspiration ([www.molinspiration.com](http://www.molinspiration.com)) based on Lipinski's (2004) "Rule of five". Furthermore, the compounds with BBB permeability were predicted via the admet structure activity relationship (SAR) server (<http://lmmd.ecust.edu.cn/admetSar1/predict/>). The data are listed in Table 2. As seen from the data, all the compounds have a high probability of crossing the BBB. None of the compounds violate Lipinski's rules, making our compounds excellent candidates as Central Nervous System (CNS)-active compounds.

#### 3.3.2 | Biological testing

##### *In vivo antihyperglycemic activity*

The *in vivo* antihyperglycemic activity of the newly synthesized Compounds 4a–d, 5a–d, 6a–d, 7a–d, 8a–d and 9a–d was examined against streptozotocin-induced hyperglycemic rats using antihyperglycemic

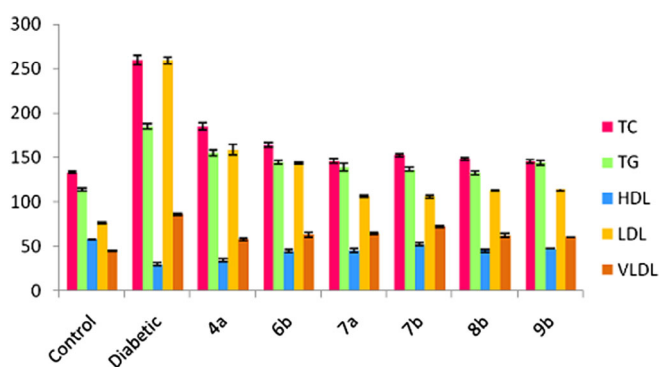


**FIGURE 6** Effect of compounds on lipid profiles (values are given as mean  $\pm$  SE)

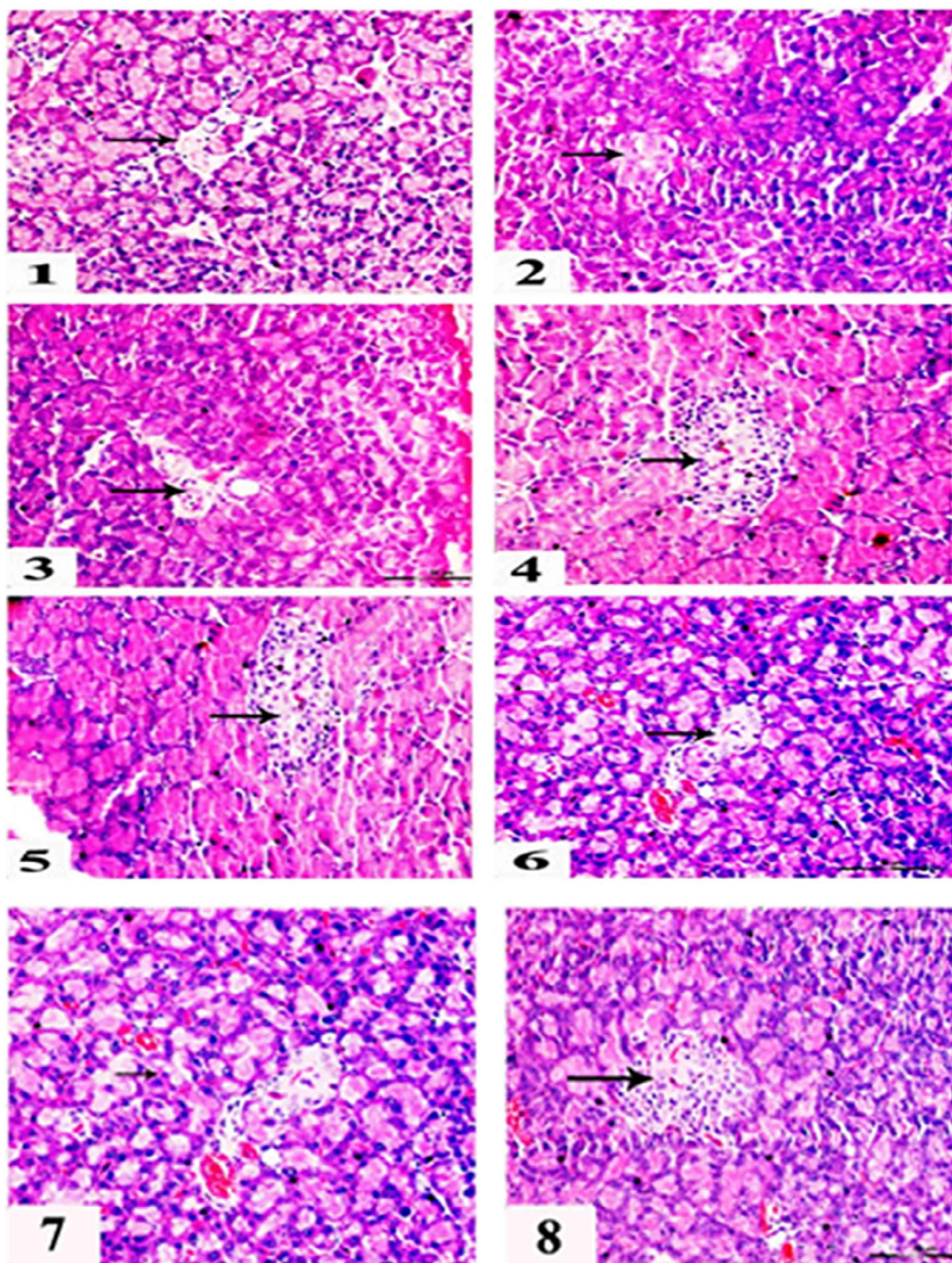


**FIGURE 7** Histology of pancreas of normal control, diabetic control, and diabetic-treated rats

assay (using Wistar albino rats of either sex having average b.w. of  $190 \pm 20$  g). Glibenclamide included in the experiment as a standard drug. The results were expressed as mg/dl reduction in blood glucose level (Table 3). Most of the synthesized molecules showed excellent to modest antihyperglycemic activity against streptozotocin-induced hyperglycemic rats.

#### *Effect of compounds on blood glucose level*

The antihyperglycemic activity of synthesized compounds was affirmed by measuring blood glucose level for 28 days. As shown in Table 3, the blood glucose levels of diabetic control rats increased significantly after the injection of streptozotocin, compared with normal (Group I) rats. Administration of Compounds 4a, 6b, 7a, 7b, 8b, and

**TABLE 6** Surflex docking score (kcal/mol) of the title Compounds 8(k-z) on enzyme glycogen phosphorylase (PDB ID: 1L5Q; B chain)

Entry no.	C-score <sup>a</sup>	Crash score <sup>b</sup>	Polar score <sup>c</sup>	D-score <sup>d</sup>	PMF score <sup>e</sup>	G-score <sup>f</sup>	Chem score <sup>g</sup>
4a	4.43	-0.96	0.33	-4,976.23	-5.70	-222.21	-30.35
6b	6.05	-2.47	2.75	-5,050.07	4.46	-247.38	-38.77
7a	4.28	-0.36	1.13	-4,828.30	-5.13	-200.51	-27.33
7b	4.48	-1.58	1.57	-4,947.20	-2.12	-234.76	-35.06
8b	4.47	-0.56	0.81	-4,729.18	9.94	-209.09	-28.55
9b	6.41	-1.79	2.17	-5,201.23	3.21	-248.45	-36.55

<sup>a</sup>C-score integrates a number of popular scoring functions for ranking the affinity of ligands bound to the active site of a receptor and reports the output of total score.

<sup>b</sup>Crash score revealing the inappropriate penetration into the binding site. Crash scores close to 0 are favorable. Negative numbers indicate penetration.

<sup>c</sup>Polar score indicating the contribution of the polar interactions to the total score. The polar score may be useful for excluding docking results that make no hydrogen bonds.

<sup>d</sup>D-score for charge and van der Waals interactions between the protein and the ligand.

<sup>e</sup>Potential of mean force (PMF) score indicating the Helmholtz free energies of interactions for protein-ligand atom pairs.

<sup>f</sup>G-score showing hydrogen bonding, complex (ligand-protein), and internal (ligand-ligand) energies.

<sup>g</sup>Chem score points for H-bonding, lipophilic contact, and rotational entropy, along with an intercept term.

**9b** daily caused gradual lowering of blood glucose level and finally reached to normal in 5–7 days which was comparable with the standard drug glibenclamide. While rats treated with other than these compounds did not show any significant decrease in blood glucose levels (<200 mg/dl).

#### Effect of compounds on SGOT, SGPT, creatinine, urea, and total protein

The SGOT and SGPT are reliable markers of liver function which are released during liver necrosis in diabetic-induced rats. An increase in the activities of SGOT and SGPT in the plasma is due to the leakage of these enzymes from the liver cytosol into the blood stream which gives the indication of hepatic dysfunctions. The serum creatinine and urea will be high in diabetic-induced rats. However, the total protein will be reduced due to insufficient insulin release which stimulates protein synthesis and retards protein degradation.

As shown in Table 4, streptozotocin-induced diabetic rats showed significant increase in SGOT, SGPT, creatinine, and urea levels, while total protein was significantly reduced. Oral administration of Compounds **4a**, **6b**, **7a**, **7b**, **8b**, and **9b** has decreased the concentrations of serum SGOT, SGPT, creatinine, and urea, and increased the total protein content in diabetic rats compared to untreated diabetic rats (Figures 4 and 5).

#### Effect of compounds on lipid profiles

DM is associated with changes in the plasma lipid profile and is considered to be major risk for coronary heart disease. In diabetic individual, LDL and VLDL carry cholesterol to the peripheral tissues where it is deposited, while HDL carry cholesterol from peripheral tissue to liver, thus facilitating its excretion and metabolism.

Entries of Table 5 indicated that in streptozotocin-induced rats, TC, TG, LDL, and VLDL levels were increased and HDL level was decreased compared to normal rats. Administration of Compounds **4a**, **6b**, **7a**, **7b**, **8b**, and **9b** showed significant reduction in elevated TC,

TG, LDL, and VLDL levels and increased HDL level compared to untreated diabetic rats (Figure 6).

#### Histopathological studies

Histology of pancreas in experimental rats was determined after 28 days of treatment. Normal control rats' normal architecture of islets of Langerhans are presented in Figure 7 (1). Diabetic control group-pancreatic sinusoid necrosis and degranulated islet cells with vanishing of nuclei resulting shrunken islets of Langerhans are presented in Figure 7 (2), diabetic rats treated with Compound **4a**, and the pancreas showing regeneration of islets of Langerhans are shown in Figure 7 (3). Diabetic rats treated with Compound **6b** and islets with beta cells containing more cytoplasm and normal exocrine acini are shown in Figure 7 (4). Diabetic rats treated with Compound **7a** and islets with beta cells containing more cytoplasm and normal exocrine acini are presented in Figure 7 (5). Diabetic rats treated with Compound **7b** and pancreas showing regeneration of islets of Langerhans are shown in Figure 7 (6). Diabetic rats treated with Compound **8b** and hence pancreas showing regeneration of islets of Langerhans are shown in Figure 7 (7). Diabetic rats treated with Compound **9b** islets with beta cells containing more cytoplasm and normal exocrine acini are presented in Figure 7 (8).

#### Structure activity relationship

As outlined in the rationale, we aimed at studying the SAR of 5-(1-aryl-1H-pyrazol-3-yl)-1H-tetrazoles **4a-d**, **5a-d**, **6a-d**, **7a-d**, **8a-d**, and **9a-d** hybrids as potential antihyperglycemic agents targeting GP enzyme. Observing the results of different in vivo biological experiments, we could presume valuable data about the SARs. The obtained results of in vivo antihyperglycemic activity in Table 4 shows that **4a-d**, **5a-d**, **6a-d**, **7a-d**, **8a-d**, and **9a-d** exhibited moderate-to-excellent antihyperglycemic activity. Among the tested compounds, Compounds **4a** (2,5-disubstituted tetrazole containing *N*-substituted *p*-

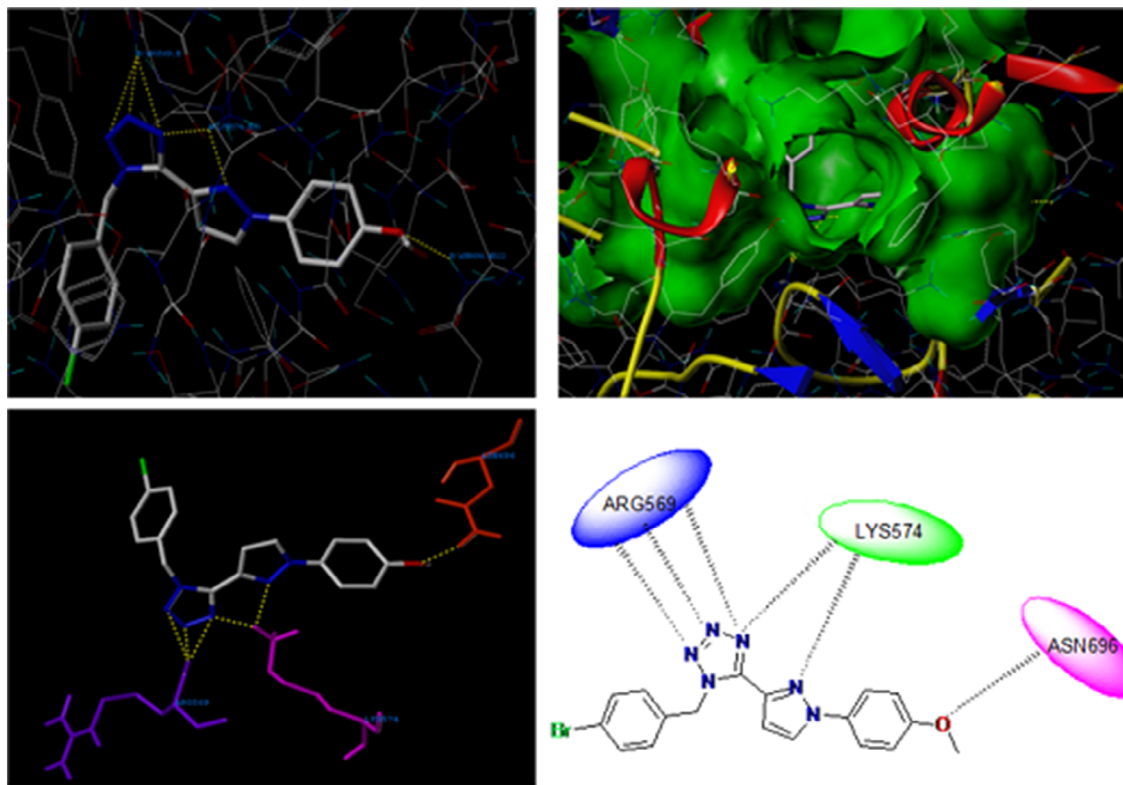


**FIGURE 8** Docked view of Compound **9b** at the active site of the enzyme glycogen phosphorylase enzyme

phenyl side chain, *N*-phenyl pyrazole), **6b** (2, 5-disubstituted tetrazole containing *N*-substituted *p*-bromobenzyl side chain, *N*-substituted *p*-anisyl pyrazole), **7a** (1,5-disubstituted tetrazole containing *N*-substituted *p*-phenyl side chain, *N*-phenyl pyrazole), **7b** (1,5-disubstituted tetrazole containing *N*-substituted *p*-bromobenzyl side chain, *N*-substituted *p*-anisyl pyrazole), **8b** (1,5-disubstituted tetrazole containing *N*-substituted *p*-bromobenzyl side chain, *N*-substituted *p*-chlorophenyl pyrazole), and **9b** (1,5-disubstituted tetrazole containing *N*-substituted *p*-bromobenzyl side chain, *N*-substituted *p*-anisyl pyrazole) have shown potent in vivo antihyperglycemic activity.

From the above results, it is clear that several 1,5-disubstituted tetrazole derivatives comprising *N*-substituted *p*-bromobenzyl side chain (viz., **6b**, **7b**, **8b**, and **9b**) have shown maximum fall in the blood glucose levels and exhibited significant decrease in SGOT, SGPT, urea, and creatinine coupled with increase in the total protein levels. Also, these compounds have exhibited antihyperlipidemic activities as evidenced by decrease in TC, TG, LDL, and VLDL coupled with the elevation of HDL levels. Moreover, the introduction of a halogen substituent at the phenyl ring resulted in enhanced antihyperglycemic activity. The rise in the in vivo activity with respect to the substituents follows the order as follows: Br > Cl > OCH<sub>3</sub> > H. Interestingly, in vivo antihyperglycemic activity revealed that the 1,5-regioisomers have shown more inhibition compared to 2,5-regioisomers representing the regioselectivity of an enzyme. These results were further confirmed by docking studies.

### 3.4 | Docking study

Docking simulation has grown to be a significant part of drug discovery analysis in the present days and it imparts information of the structural and functional aspects of proteins and ligands. In this regard, with in vivo antihyperglycemic activity results in hand, it was appropriate to carry out in silico studies to support the in vivo activity. The potent antihyperglycemic compounds, namely, **4a**, **6b**, **7a**, **7b**, **8b**, and **9b** were docked into the active site of the GP (PDB ID: 1L5Q; B chain). The predicted binding energies and the observed consensus score (C-score) values of potent molecules are ranging from 4.28 to 6.41 (Table 6). The C-score values representing the summary of all forces of interaction between ligands and the GP. It may be concluded that all potent compounds have exhibited very good docking score against target enzyme.

Among docked compounds, Compound **9b** acts as very good inhibitor of GP enzyme. As depicted in Figure 8, Compound **9b** makes six hydrogen bonding interaction at the active site of the enzyme (PDB ID: 1L5Q; B chain), among them four interactions came from the tetrazole ring, out of which three hydrogen bonding interactions were raised from nitrogen atoms of tetrazole ring with hydrogen of ARG569 (—N···H-ARG569) and another one with hydrogen of LYS574 (—N···H-LYS574). Also, nitrogen atom of pyrazole ring makes a hydrogen bonding interaction with hydrogen of LYS574 (—N···H-LYS574), and oxygen atom of methoxy group present at the fourth position of aromatic ring makes hydrogen

bonding interaction with hydrogen of ASN696 ( $-\text{OCH}_3 \cdots \text{H}-\text{ASN696}$ ).

## 4 | CONCLUSIONS

In summary, we herein report the ring transformation of 3-arylsydnone into 1-aryl-1H-pyrazole-3-carbonitriles via [3 + 2] cycloaddition reaction which was then converted to 5-(1-aryl-1H-pyrazol-3-yl)-1H-tetrazole. N-Alkylation of 5-(1-aryl-1H-pyrazol-3-yl)-1H-tetrazole afforded 1,5- and 2,5-disubstituted regioisomeric tetrazoles which were separated by column chromatographic technique. Our pharmacokinetic study verified the potential of the synthesized molecules as novel drug-like candidates and considers these molecules as lead targets for further progress in drug discovery process. The in vivo antihyperglycemic activity assay revealed that Compounds **4a**, **6b**, **7a**, **7b**, **8b**, and **9b** have helped significantly in lowering the blood glucose levels and in prevention of vascular complications in streptozotocin-induced diabetic rats. The administration of Compounds **4a**, **6b**, **7a**, **7b**, **8b**, and **9b** daily for 28 days to streptozotocin-induced diabetic rats has resulted significant decrease in SGOT, SGPT, urea, and creatinine coupled with increase in the total protein levels. Also, these compounds have exhibited antihyperlipidemic activities as evidenced by decrease in TC, TG, LDL, and VLDL coupled with elevation of HDL levels. The results of histopathology (pancreas) of diabetic rats when treated with Compounds **4a**, **6b**, **7a**, **7b**, **8b**, and **9b** have shown significant regeneration of islets of Langerhans with more cytoplasm and beta cells. Furthermore, the in silico docking studies were performed to analyze the binding mode of these compounds. Thus, docking results almost equalize with actual experimental in vivo findings.

## ACKNOWLEDGMENTS

The authors acknowledge UGC, New Delhi, for the financial assistance under the UPE program vide no. F.No. 14-3/2012 (NS/PE) (dated: March 14, 2012) and DSA: F-540/2/DSA/2013 (SAP-1).

## CONFLICT OF INTEREST

The authors declare no potential conflict of interest.

## AUTHOR CONTRIBUTIONS

P.P.K. and R.R.K. devised the project, the main conceptual ideas, and proof outline. R.R.K. supervised the project. P.P.K. and R.R.K. designed and synthesized the molecules. S.M.S., P.K.B., and R.K.H. helped to supervise the project and analyzed the experimental data. S.C.B. performed the in vivo antihyperglycemic activity and biochemical tests. S.D.J. conducted the molecular docking study. P.P.K., R.R.K., S.M.S., P.K.B. wrote the manuscript with input from all authors. All authors provided critical feedback and helped shape the research, analysis and manuscript.

## ORCID

Ravindra R. Kamble  <https://orcid.org/0000-0002-0384-655X>

## REFERENCES

- Abdel-Aziz, M., El-Din, A., Abu-Rahma, G., & Hassan, A. A. (2009). Synthesis of novel pyrazole derivatives and evaluation of their antidepressant and anticonvulsant activities. *European Journal of Medicinal Chemistry*, *44*, 3480–3487.
- Al-Hourani, B. J., Sharma, S. K., Mane, J. Y., Tuszyński, J., Baracos, V., Kniess, T., ... Wuest, F. (2011). Synthesis and evaluation of 1,5-diaryl-substituted tetrazoles as novel selective cyclooxygenase-2 (COX-2) inhibitors. *Bioorganic Medicinal Chemistry Letters*, *21*, 1823–1826.
- Altıntop, M. D., Ozdemir, A., Ilgin, S., & Atli, O. (2014). Synthesis and biological evaluation of new pyrazole-based thiazolyl hydrazone derivatives as potential anticancer agents. *Letters in Drug Design & Discovery*, *11*(7), 833–839.
- Angadiyavar, C. S., & George, M. V. (1971). Photochemical cycloadditions of 1,3-dipolar systems. I. Additions of N,C-diphenylsydnone and 2,5-diphenyltetrazole. *Journal of Organic Chemistry*, *36*, 1589–1594.
- Arshad, M., Bhat, A. F., Pokharel, S., Kim, J. E., Lee, E. J., Athar, F., & Choi, I. (2014). Synthesis, characterization and anticancer screening of some novel piperonyl-tetrazole derivatives. *European Journal of Medicinal Chemistry*, *71*, 229–236.
- Ashton, W. T., Cantone, C. L., Meurer, L. C., Tolman, R. L., Greenlee, W. J., Patchett, A. A., ... Siegl, P. K. S. (1992). Renin inhibitors containing C-termini derived from mercaptoheterocycles. *Journal of Medicinal Chemistry*, *35*, 2103–2112.
- Baker, D. J., Greenhaff, P. L., & Timmons, J. A. (2006). Glycogen phosphorylase inhibition as a therapeutic target: a review of the recent patent literature. *Expert Opinion on Therapeutic Patents*, *16*, 459–466.
- Browne, D. L., & Harrity, J. P. A. (2010). Recent developments in the chemistry of sydnones. *Tetrahedron*, *66*, 553–568.
- Bruker. (2001). *SMART and SAINT*. Madison, WI: Bruker AXS Inc.
- Butler, R. N. (1996). Tetrazoles. In A. R. Katritzky, C. W. Rees, & S. EFV (Eds.), *Comprehensive heterocyclic chemistry II* (Vol. 4, pp. 621–678). Oxford: Pergamon Press.
- Chang, C. S., Lin, Y. T., Shih, S. R., Lee, C. C., Lee, Y. C., Tai, C. L., ... Chern, J. H. (2005). Design, synthesis, and anticoronavirus activity of 1-[5-(4-arylphenoxy) alkyl]-3-pyridin-4-ylimidazolidin-2-one derivatives. *Journal of Medicinal Chemistry*, *48*, 3522–3535.
- Diamond, J. (2003). The double puzzle of diabetes. *Nature*, *423*, 599–602.
- El-Sabbagh, O. I., Baraka, M. M., Ibrahim, S. M., Pannecouque, P., Andrei, G., Snoeck, R., ... Rashad, A. A. (2009). Synthesis and antiviral activity of new pyrazole and thiazole derivatives. *European Journal of Medicinal Chemistry*, *44*, 3746–3753.
- Farrugia, L. J. (2012). WinGX and ORTEP for Windows: An update. *Journal of Applied Crystallography*, *45*, 849–854.
- Friedewald, W. T., Levy, R. I., & Fredrickson, D. S. (1972). Estimation of the concentration of low-density lipoprotein cholesterol in plasma, without use of the preparative ultracentrifuge. *Clinical Chemistry*, *18*, 499–502.
- Fujimori, Y., Katsuno, K., Nakashima, I., Ishikawa-Takemura, Y., Fujikura, H., & Isaji, M. (2008). Remogliflozin etabonate, in a novel category of selective low-affinity sodium glucose cotransporter (SGLT2) inhibitors, exhibits antidiabetic efficacy in rodent models. *Journal of Pharmacology and Experimental Therapeutics*, *327*, 268–276.
- Gao, Y. L., Zhao, G. L., Liu, W., Shao, H., Wang, Y. L., Xu, W. R., ... Wang, J. W. (2010). Design, synthesis and in vivo hypoglycemic activity of tetrazole-bearing N-glycosides as sglT2 inhibitor. *Indian Journal of Chemistry*, *49B*, 1499–1508.

- Gasteiger, J., & Marsili, M. (1980). Iterative partial equalization of orbital electronegativity—A rapid access to atomic charges. *Tetrahedron*, *36*, 3219–3228.
- Henke, B. R., & Sparks, S. M. (2006). Glycogen phosphorylase inhibitors. *Mini-Reviews in Medicinal Chemistry*, *6*, 845–857.
- Hoover, D. J., Lefkowitz-Snow, S., Burgess-Henry, J. L., Martin, W. H., Armento, S. J., Stock, I. A., ... Treadway, J. L. (1998). Indole-2-carboxamide inhibitors of human liver glycogen phosphorylase. *Journal of Medicinal Chemistry*, *41*, 2934–2938.
- IDF Diabetes Atlas. Retrieved from: <http://www.idf.org/diabetesatlas2018>.
- Karabanovich, G., Roh, J., Soukup, O., Pavkova, I., Pasdiorova, M., Tamboor, V., ... Hrabalek, A. (2015). Tetrazole regioisomers in the development of nitro group-containing antitubercular agents. *Medicinal Chemistry Communications*, *6*, 174–181.
- Kothayer, H., Ibrahim, S. M., Soltan, M. K., Rezaq, S., & Mahmoud, S. S. (2018). Synthesis, in vivo and in silico evaluation of novel 2,3-dihydroquinazolin-4(1H)-one derivatives as potential anticonvulsant agents. *Drug Development Research*, *80*, 1–10.
- Kurukulasuriya, R., Link, J. T., Madar, D. J., Pei, Z., Richards, S. J., Rohde, J. J., ... Szczepankiewicz, B. G. (2003). Potential drug targets and progress towards pharmacologic inhibition of hepatic glucose production. *Current Medicinal Chemistry*, *10*, 123–153.
- Le Bourdonnec, B., Meulon, E., Yous, S., Goossens, J. F., Houssin, R., & Henichart, J. P. (2000). Synthesis and pharmacological evaluation of new pyrazolidine-3,5-diones as AT<sub>1</sub> angiotensin II receptor antagonists. *Journal of Medicinal Chemistry*, *43*, 2685–2697.
- Lipinski, C. A. (1986). Bioisosterism in drug design. *Annual Reports in Medicinal Chemistry*, *21*, 283–291.
- Loughlin, W. A. (2010). Recent advances in the allosteric inhibition of glycogen phosphorylase. *Mini-Reviews in Medicinal Chemistry*, *10*, 1139–1155.
- Mallur, S. G., & Badami, B. V. (2000). Transformation of the sydnone ring into oxadiazolinones. A convenient one-pot synthesis of 3-aryl-5-methyl-1,3,4-oxadiazolin-2-ones from 3-arylsydnones and their antimicrobial activity. *Farmaco*, *55*, 65–67.
- Matschinsky, F. M. (1996). Banting Lecture 1995. A lesson in metabolic regulation inspired by the glucokinase glucose sensor paradigm. *Diabetes*, *45*, 223–241.
- May, B. C. H., & Abell, A. D. (2001). The synthesis and crystal structure of alpha-keto tetrazole-based dipeptide mimics. *Tetrahedron Letters*, *42*, 5641–5644.
- May, B. C. H., & Abell, A. D. (2002).  $\alpha$ -Methylene tetrazole-based peptidomimetics: Synthesis and inhibition of HIV protease. *Journal of the Chemical Society, Perkin Transactions*, *1*(1), 172–178.
- Muraglia E., Kinzel O.D., Laufer R., Miller M.D., Moyer G., Munshi V., Orvieto F., Palumbi M.C., Pescatore G., (2006). Rowley M., Williams P. D., Summa V., Tetrazole thioacetanilides: potent non-nucleoside inhibitors of WT HIV reverse transcriptase and its K103N mutant. *Bioorganic Medicinal Chemistry Letters*, *16*, 2748–2752.
- Nisa, M.-U., Munavar, M. A., Chattha, F. A., Kousar, S., Munir, J., Ismail, T., ... Khan, M. A. (2015). Synthesis of novel triazoles and a tetrazole of escitalopram as cholinesterase inhibitors. *Bioorganic Medicinal Chemistry*, *23*, 6014–6024.
- Oikonomakos, N. G. (2002). Glycogen phosphorylase as a molecular target for type 2 diabetes therapy. *Current Protein & Peptide Science*, *3*, 561–586.
- Oikonomakos, N. G., & Somsák, L. (2008). Advances in glycogen phosphorylase inhibitor design. *Current Opinion in Investigational Drugs*, *9*, 379–395.
- Pandey, S., Agarwal, P., Srivastava, K., Rajakumar, S., Puri, S. K., Verma, P., ... Chauhan, P. M. S. (2013). Synthesis and bioevaluation of novel 4-aminoquinoline-tetrazole derivatives as potent antimalarial agents. *European Journal of Medicinal Chemistry*, *66*, 69–81.
- Pedro, A. C., Alejandro, I. J., Joaquin, G. M., Lilian, Y. M., Fernando, C., & Rocio, G. M. (2014). Synthesis of 3-tetrazolymethyl-4H-chromen-4-ones via Ugi-azide and biological evaluation against *Entamoeba histolytica*, *Giardia lamblia* and *Trichomonas vaginalis*. *Bioorganic Medicinal Chemistry*, *22*, 1370–1376.
- Raffa, D., Migliara, O., Maggio, B., Plescia, F., Cascioferro, S., Cusimano, M. G., ... Plescia, F. (2010). Pyrazolobenzotriazinones derivatives as COX inhibitors: synthesis biological activity and molecular modeling studies. *Archiv der Pharmazie Chemie in Life Sciences*, *10*, 631–638.
- Rajasekaran, A., & Thampi, P. P. (2004). Synthesis and analgesic evaluation of some 5-[b-(10-phenothiazinyl)ethyl]-1-(acyl)-1,2,3,4-tetrazoles. *European Journal of Medicinal Chemistry*, *39*, 273–279.
- Reitman, S., & Frankel, S. (1957). A colorimetric method for the determination of serum glutamic oxalacetic and glutamic pyruvic transaminases. *American Journal of Clinical Pathology*, *28*, 56–63.
- Ren, Z. L., Liu, H., Jiao, D., Hu, H. T., Wang, W., Gong, J. X., ... Lv, X. H. (2018). Design, synthesis, and antifungal activity of novel cinnamopyrazole carboxamide derivatives. *Drug Development Research*, *79*, 307–312.
- Rostom, S. A. F., Ashour, H. M. A., Abd El Razik, H. A., Abd El Fattah, A. E. H., & El-Din, N. N. (2009). Azole antimicrobial pharmacophore-based tetrazoles: Synthesis and biological evaluation as potential antimicrobial and anticonvulsant agents. *Bioorganic Medicinal Chemistry*, *17*, 2410–2422.
- Sharon, A., Pratap, R., Tiwari, P., Srivastava, A., Maulik, P. R., & Ram, V. J. (2005a). 6-Aryl-4-methylsulfanyl-2H-pyran-2-one-3-carbonitriles as PPAR-gamma activators. *Bioorganic Medicinal Chemistry Letters*, *15*, 3356–3360.
- Sharon, A., Pratap, R., Tiwari, P., Srivastava, A., Maulika, P. R., & Ram, V. J. (2005b). Synthesis and in-vivo antihyperglycemic activity of 5-(1H-pyrazol-3-yl) methyl-1H-tetrazoles. *Bioorganic Medicinal Chemistry Letters*, *15*, 2115–2117.
- Sheldrick, G. M. (1997). *SHELXL97*. Gottingen, Germany: University of Gottingen.
- Singh, P., Paul, K., & Holzer, W. (2006). Synthesis of pyrazole e based hybrid molecules: search for potent multidrug resistance modulators. *Bioorganic Medicinal Chemistry*, *14*, 5061–5071.
- Somsak, L., Czifrak, K., Toth, M., Bokor, E., Chrysin, E. D., Alexacou, K.-M., ... Oikonomakos, N. G. (2008). New inhibitors of glycogen phosphorylase as potential antidiabetic agents. *Current Medicinal Chemistry*, *15*, 2933–2983.
- Sridhar, R., Perumal, P. T., Etti, S., Shanmugam, G., Ponnuswamy, M. N., Prabavathy, V. R., & Mathivanan, N. (2004). Design, synthesis and anti-microbial activity of 1H-pyrazolecarboxylates. *Bioorganic & Medicinal Chemistry Letters*, *4*, 6035–6040.
- Subramanian, V., Knight, J. S., Parekar, S., Anguish, L., Coonrod, S. A., Kaplan, M. J., & Thompson, P. R. (2015). Design, synthesis, and biological evaluation of tetrazole analogs of Cl-amidine as protein arginine deiminase inhibitors. *Journal of Medicinal Chemistry*, *58*, 1337–1344.
- Tiwari, U., Ameta, C., Ranwal, M. K., Ameta, R., & Punjabi, P. B. (2013). MW assisted synthesis of some pyrazoles containing benzotriazole moiety: An environmentally benign approach. *Indian Journal of Chemistry-Section B*, *52*, 432–439.
- Treadway, J. L., Mendys, P., & Hoover, D. J. (2001). Glycogen phosphorylase inhibitors for treatment of type 2 diabetes mellitus. *Expert Opinion on Therapeutic Patents*, *10*, 439–454.
- Tripos International. (2012). *Sybyl-X 2.0*. St. Louis, MO: Author.
- Uchida, M., Komatsu, M., Morita, S., Kanbe, T., Yamasaki, K., & Nakagawa, K. (1989). Studies on gastric antiulcer active agents. III. Synthesis of 1-substituted 4-(5-tetrazolyl)thio-1-butanones and related compounds. *Chemical & Pharmaceutical Bulletin (Tokyo)*, *37*, 958–961.

- Vieira, E., Huwlyer, J., Jolidon, S., Knoflach, F., Mutel, V., & Wichmann, J. (2005). 9H-Xanthene-9-carboxylic acid [1,2,4]oxadiazol-3-yl- and (2H-tetrazol-5-yl)-amides as potent, orally available mGlu1 receptor enhancers. *Bioorganic Medicinal Chemistry Letters*, 15, 4628–4631.
- Wagman, A. S., & Nuss, J. M. (2001). Current therapies and emerging targets for the treatment of diabetes. *Current Pharmaceutical Design*, 7, 417–450.
- Wittenberger, S. J. (1994). Recent developments in tetrazole chemistry: A review. *Organic Preparations and Procedures International*, 26, 499–531.
- World Health Organization. Global Report on Diabetes. Author: Geneva, 2016. Retrieved from: <http://www.who.int/diabetes/global-report/en/>.
- Wu, C., Fang, Y., Larock, R. C., & Shi, F. (2010). Synthesis of 2H-indazoles by the [3+2] cycloaddition of arynes and sydrones. *Organic Letters*, 12, 2234–2237.
- Zhang, G. Y. (2009). N-(5-Methylsulfanyl-1,3,4-thiadiazol-2-yl)acetamide. *Acta Crystallographica*, E65, o2138.
- Zimmet, P., Alberti, K. G., & Shaw, J. (2001). Global and societal implications of the diabetes epidemic. *Nature*, 414, 782–861.

#### SUPPORTING INFORMATION

Additional supporting information may be found online in the Supporting Information section at the end of this article.

**How to cite this article:** Kattimani PP, Somagond SM, Bayannavar PK, et al. Novel 5-(1-aryl-1H-pyrazol-3-yl)-1H-tetrazoles as glycogen phosphorylase inhibitors: An in vivo antihyperglycemic activity study. *Drug Dev Res*. 2019;1–15. <https://doi.org/10.1002/ddr.21606>